procedures. *Int. J. Rock Mech. Min. Sci. Geomech. Abstr.*, 1996, **33**, 189–196.
23. Latham, J. P., Munjiza, A. and Lu, P., Components in an understanding of rock blasting. In Proceedings of the Sixth International Symposium on Rock Fragmentation by Blasting, Johannesburg, South Africa, 1999, pp. 173–182.
24. Jhanwar, J. C., Jethwa, J. L. and Reddy, A. H., Influence of air-deck blasting on fragmentation in jointed rocks in an open-pit manganese mine. *Eng. Geol.*, 2000, **57**, 13–29.
25. Sanchidrian, J. A., Segarra, P. and Lopez, M. L., Energy components in rock blasting. *Int. J. Rock Mech. Mining Sci.*, 2007, **44**, 130–147.
26. Engin, I. C., A practical method of bench blasting design for desired fragmentation based on digital image processing technique and Kuz–Ram model. In Proceedings of the Ninth International Symposium on Rock Fragmentation by Blasting, Granada, Spain, 2009, pp. 257–263.
27. Dozolme, P., Back to basics on rock fragmentation, 2014; On-line access: http://mining.about.com/od/SurfaceMining101/a/Back-To-Basics-On-rockFragmentation.htm
28. Jimeno, C. L., Jimeno, E. L. and Carcedo, F. J. A., *Drilling and Blasting of Rocks*, Rotterdam, Balkema, 1995.
29. Scott, A., Blastability and blast design. In Fifth International Conference on Rock Fragmentation by Blasting (ed. Mohanty, B.), Montreal, Canada, 1996, pp. 27–36.
30. Scott, A., Cocker, A., Djordjevic, N., Higgins, M. La., Rosa, D., Sarma, K. S. and Wedmaier, R., Open pit blast design, analysis and optimization. In Julius Kruttschnitt Mineral Research Centre, Queensland, Australia, 1999, p. 338.
31. Seppälä, A., Development of blasting design to optimize fragmentation by analysing drilling accuracy and loading capacities in the open pit mine Talvivaara Master's thesis, Aalto University, Greater Helsinki, Finland, 2011.
32. Medvedev, A. E., Fomin, V. M. and Reshetnyak, A. Yu., Mechanism of detonation of emulsion explosives with microballoons. *Shock Waves*, 2008, **18**, 107–115.
33. Persson, P. A., Holmberg, R. and Lee, J., *Rock Blasting and Explosives Engineering*, CRC, Boca Raton, USA, 2001, p. 541.
34. Leidig, M., Bonner, J. L., Rath, T. and Murray, D., Quantification of ground vibration differences from well-confined single-hole explosions with variable velocity of detonation. *Int. J. Rock Mech. Min. Sci.*, 2010, **47**, 42–49.
35. Konya, C. J. and Walter, E. J., Rock blasting and overbreak control, FHWA Report FHWA-HI-92-101, 1991.
36. WipFrag, User manual; http://wipware.com/PDFs-manuals

Received 24 June 2015; accepted 8 August 2016

doi: 10.18520/cs/v112/i03/602-608

Record of post-collisional A-type magmatism in the Alwar complex, northern Aravalli orogen, NW India

Parampreet Kaur*, Nusrat Eliyas and Naveen Chaudhri*

Centre of Advanced Study in Geology, Panjab University, Chandigarh 160 014, India

The Alwar complex is situated in the northern part of the Aravalli orogen, NW India and contains A-type granites of late Palaeoproterozoic age. The current study focusses on the Harsora and Dadikar plutons to characterize and constrain the tectonic setting of Palaeoproterozoic felsic A-type magmatism in this crustal segment using whole-rock geochemical data. The rocks studied are metaluminous to slightly peraluminous A-type ferroan granites. The granites are generally characterized by strongly fractionated LREE patterns with nearly flat HREE profiles and show moderate to strong negative Eu anomalies, in addition to prominent negative anomalies in Ba, Nb, Sr, P and Ti. The results show the post-collisional setting of A-type granites in the northern Aravalli orogen and signify that A-type granites may not only form in anorogenic setting. This study provides a new dimension to the understanding of palaeoproterozoic geodynamic evolution in the Aravalli orogen.

Keywords: A-type granites, post-collision, Aravalli orogen, Alwar complex, whole-rock geochemistry.

GRANITOIDS form one of the most common components of the continental crust[1,2], especially in Precambrian terrains. Knowledge of nature and genesis of granitoids is, therefore, crucial for understanding the evolution of any crustal block. Based on chemistry and petrography, granitoids are usually classified into I-S-M and A-types[3–5]. The term A-type granite was introduced by Loiselle and Wones[4] for a specific suite of granitoids, which are anhydrous, alkaline and anorogenic[6,7]. A-type granites occur in a number of regionally extension-related environments, such as continental rift zones, post-collisional setting, and even in subduction-related settings[4,7–11]. Therefore, they provide significant information on the extensional magmatic processes that contribute to the chemical evolution of upper continental crust[10,12].

In the northern Aravalli orogen, a number of A-type intrusions occur in two igneous-metamorphic complexes, designated as the Alwar complex[13–15] and the Khetri complex[16–20], also known as the Alwar basin or the Khetri basin. These rocks are late Palaeoproterozoic spanning an age range of 1.72–1.70 Ga (refs 14, 18, 19, 21). However,

*For correspondence. (e-mail: param.geol@gmail.com; naveen.geol@gmail.com)

the tectonic setting of these rocks is not well constrained, except for some passing references that these are anorogenic[13,16]. This information is, nevertheless, critical to comprehend the geodynamic evolution of the Aravalli orogen. The present study deals with geochemical investigations on two A-type plutons (Harsora and Dadikar) from the Alwar complex of northern Aravalli orogen, and these granites were generated in a post-collisional extension setting.

The Alwar complex is covered by the rocks of Delhi Supergroup, and these rocks in the complex are stratigraphically classified into an older Raialo Group, overlain by the Alwar Group and the younger Ajabgarh Group[22,23] (Figure 1). The rocks of Raialo Group are predominantly carbonates with quartzite and metavolcanics. The Alwar and Ajabgarh Groups are dominantly characterized by arenaceous and argillaceous rocks respectively. The rocks show polyphase deformation, and three main folding phases have been recognized[24]. The first phase of deformation produced a series of moderate to shallow plunging NNE-SSW trending isoclinal folds (F_1). These were subsequently refolded into a set of folds (F_2) with steep or vertical axial planes. These two generations of folds are co-axial and their interference has resulted in a 'hook-shaped' geometry. The latest generation of folds (F_3) is represented by broad wrap gentle folds and kink bands. These folds have sub-vertical plunge with WNW–ESE trending axial planes. The metamorphism in the region resembles a type between Barrovian and Abukuma, and has been estimated to took place at 500–550°C temperature and 300–400 MPa pressure[25,26]. The type of fold geometry and style, and the metamorphic history of the Alwar complex are apparently identical to that of the Khetri complex[27–32].

The igneous rocks, occurring in the area, are represented by mafic sills and dykes, granitoids and pegmatites[14,33]. The granitoid rocks of Dadikar and Harsora plutons are located in the NW of Alwar town (Figure 1). Biju-Sekhar *et al.*[14] classified these granitoids as A-type granites and also reported their ages by zircon EPMA method at 1780–1726 Ma.

The Harsora pluton is exposed amidst alluvium and quaternary sand as an elongated body. Its maximum present day dimension is 8 × 5 km, and due to sand cover, it is not possible to study the contact relationship between the granite and the Delhi rocks. The majority of the pluton is made up of grey to greyish pink granitoids, which are well-foliated (Figure 2 *a*) in a NE-SW direction with easterly dips of 45–64°. It is largely a two-feldspar granite with biotite or amphibole or both as the major minerals. The biotite and amphibole are Fe-rich annite (average X_{Fe} = 0.73–0.82) and hastingsite (average X_{Fe} = 0.89–0.96; Kaur *et al.* unpublished data). Another subordinate variety is a non-foliated, white albite granite with negligible mafic minerals. This variety is identical to the extremely metasomatized albite granites of the Ajitgarh pluton and also those of the Khetri complex[15,20,34]. This granitoid type is not considered for magmatic characterization in the present study as such rocks provide misleading interpretation[20]. The Dadikar pluton is an oval-shaped body elongated in NE–SW direction, and is enveloped on all sides by the Delhi metasedimentary rocks, dominantly quartzite with minor marble (Figure 2 *b*). Its dimensions, at the current level of exposure, are 5.25 × 4.25 km. The quartzite is considered to be part of the Alwar Group[33]. The Dadikar pluton along with the country rocks form a large-scale dome with ends tapering towards northeast and southwest directions, and has a relatively wider central part[33]. The contact between granite and quartzite is delineated by a zone of deformed conglomerate (Figure 2 *c*). The lack of any intrusive relationship between granite and quartzite, but occurrence of conglomerate between them, indicates the basement nature of the granite. This interpretation supports the finding of Biju-Sekhar *et al.*[14] who proposed that A-type granites in the Alwar complex formed basement for the Delhi sedimentation. Similarly, based on field observations and U–Pb detrital zircon age data from the Alwar quartzite, Kaur *et al.*[35] advocated that the Khetri A-type granites formed the basement for sedimentation of the Delhi rocks. These workers also reported the occurrence of sedimentary breccia and deformed conglomerate at the contact of the country rocks and A-type granites of the Khetri complex[15,20]. The Dadikar pluton is also comprised of similar varieties of

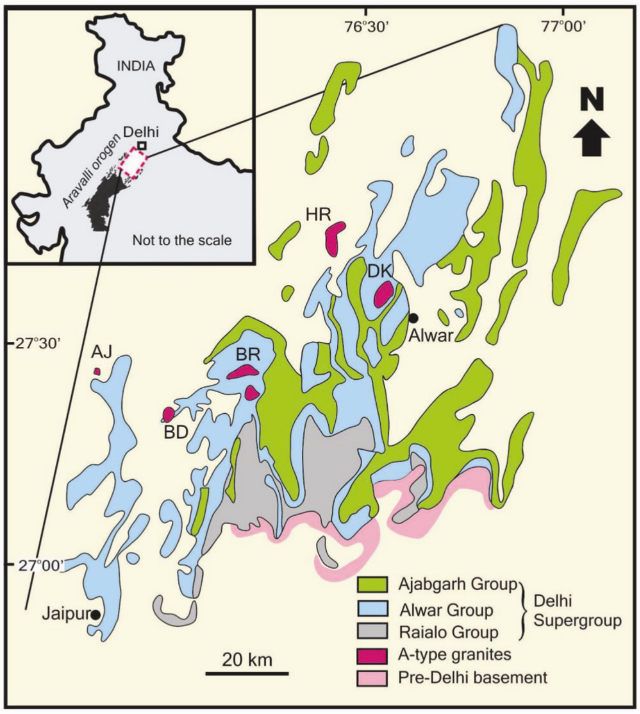

Figure 1. Geological map of the Alwar complex showing major lithological units, including the occurrences of A-type granites (modified after Singh[55]). AJ: Ajitgarh, BD: Barodia, BR: Bairat, DK: Dadikar and HR: Harsora.

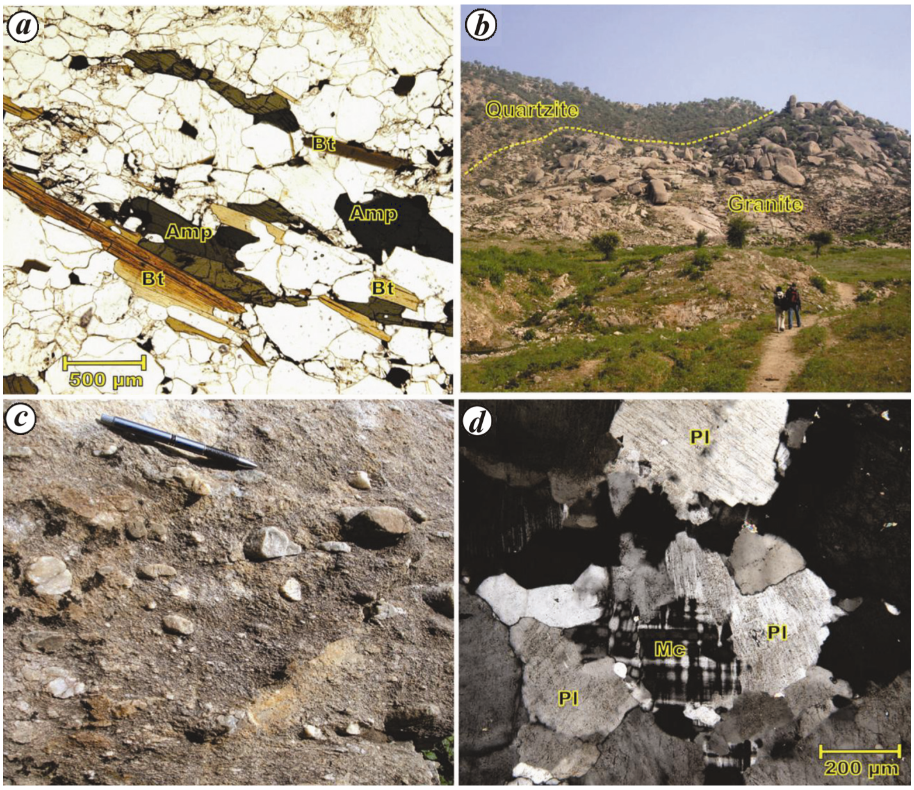

Figure 2. Representative field and photomicrographs of the Harsora and Dadikar plutons, showing: ***a***, biotite and amphibole defining foliation in the Harsora granite (plane polarized light); ***b***, Dadikar granite and the enveloping quartzite; ***c***, deformed conglomerate at the contact between the Dadikar granite and quartzite; the length of the pen is about 14 cm; ***d***, overall view of the Dadikar granite showing plagioclase and microcline with diffused margins (cross nicols).

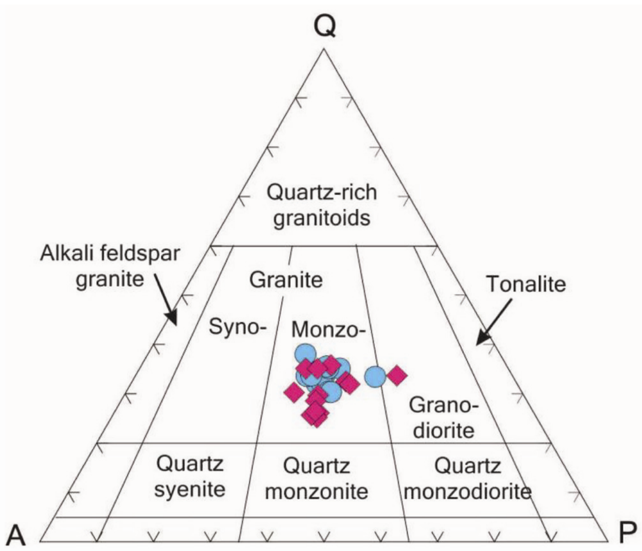

Figure 3. QAP classification diagram of Streckeisen[36] showing CIPW normative compositions of the Harsora and Dadikar granites.

the granitoids (Figure 2 *d*) with the same mineralogy as that of the Harsora pluton.

Whole-rock elemental data for granitoids under consideration were obtained from Activation Laboratories Ltd (for details see www.actlabs.com), and are presented in Table 1. A number of international rock standards, such as BCR2, W2a, JR1, DNC1, BIR1a, SY4, etc. were used to monitor the accuracy of the analyses. Duplicate measurements of samples 2HR-24 yielded a precision of <1 to 4% (SD, standard deviation) for trace and rare earth elements, except for V (9%) and Nb (6%). It is ≤1.5% for major elements, except for MgO (1.9%). In the CIPW-normative QAP ternary diagram (Figure 3) given by Streckeisen[36], most samples occupy the field of granite (monzo) and are thus classified as granite *sensu stricto*. This classification is also confirmed by the normative Ab–Or–An compositions[37] (Figure not shown). The average Si contents in the granites is >70 wt%, indicating that the rocks are evolved. The major element abundances in both plutons are similar, although Harsora granites tend to be relatively poor in alkalis (av. Na_2O = 2.92 wt% and av. K_2O = 5.07 wt% in the Harsora granites and av. Na_2O = 3.24 wt% and av. K_2O = 5.28 wt% in the Dadikar granites). Also, the Dadikar granites show more enrichment in Zr, Th and Hf abundances than the Harsora counterparts. The total REE abundances are greater in Dadikar compared to Harsora. The granites display variably fractionated REE profiles (Figure 4 *a*); the REE patterns for the Dadikar granites are more strongly

Table 1. Representative whole-rock chemical compositions for the Harsora and Dadikar granites, northern Aravalli orogen, NW India

	Harsora granite						Dadikar granite				
Sample no.	HR-1	HR-7	HR-16	HR-20	2HR-24	2HR-31	DK-8	DK-9	DK-10	2DK-19	2DK-28
SiO_2	71.82	74.76	73.65	73.05	73.52	69.38	74.30	73.37	76.18	73.15	74.93
TiO_2	0.34	0.06	0.18	0.31	0.40	0.54	0.14	0.25	0.09	0.29	0.20
Al_2O_3	13.04	12.68	12.84	12.89	12.81	13.19	11.95	13.37	12.61	12.47	12.89
$Fe_2O_3^t$	3.46	1.17	1.78	3.05	3.45	5.18	2.16	2.90	1.11	3.09	2.48
MnO	0.04	0.01	0.01	0.03	0.04	0.07	0.01	0.02	0.005	0.03	0.02
MgO	0.35	0.05	0.19	0.37	0.34	0.60	0.11	0.24	0.05	0.20	0.16
CaO	1.52	0.78	0.98	1.43	1.62	2.15	0.73	1.24	0.86	1.20	1.10
Na_2O	2.79	3.20	2.87	2.89	3.03	2.77	2.94	3.55	3.37	3.87	2.99
K_2O	5.07	5.34	5.69	5.03	4.75	5.00	5.57	4.66	4.98	4.53	5.31
P_2O_5	0.10	0.03	0.04	0.09	0.09	0.13	0.04	0.06	0.01	0.07	0.09
LOI	0.52	0.52	0.55	0.60	0.60	0.70	0.62	0.60	0.73	0.66	0.59
Sum	99.05	98.61	98.78	99.75	100.70	99.69	98.58	100.30	100.00	99.57	100.80
V	7	7	5	7	6	10	2	4	1	4	2
Cr	18	18	9	17	13	30	<5	14	<5	9	7
Co	<20	<20	<20	<20	<20	<20	<20	<20	<20	<20	<20
Ni	24	25	26	26	22	21	24	17	23	22	22
Zn	<20	<20	<20	<20	<20	<20	<20	<20	<20	<20	<20
Ga	<30	<30	<30	<30	<30	40	<30	<30	<30	<30	<30
Rb	20	20	18	18	20	19	22	21	20	22	21
Sr	343	270	398	305	278	251	251	237	358	232	312
Y	57	73	32	55	68	78	26	69	25	44	40
Zr	54	58	82	52	51	50	53	54	47	76	39
Nb	213	322	152	192	295	293	219	251	110	362	207
Ba	9	14	11	8	14	14	10	12	14	18	12
Pb	482	734	211	470	639	717	187	404	75	388	218
Th	21	28	24	18	34	23	39	27	52	28	47
U	43	48.7	85.2	41.7	48.7	34.4	112	44.5	61.5	47.9	101
Hf	12.9	13.2	23.2	9.1	11.6	7.8	14.1	9.1	16.5	5.2	16
Ta	5.4	8.1	5.2	5	7.4	7.6	7.1	7.2	4.5	10.4	7
La	78.6	46	97.3	73.2	85.1	66.8	224	87.2	35.8	98.7	129
Ce	154	99.6	185	144	168	130	402	164	71.8	197	230
Pr	16.5	11.8	19	15.6	16.7	14.4	37.1	17.3	7.46	22.6	20.8
Nd	57.1	44.5	62.7	53.2	56.4	51.9	112	56.6	24.6	81.9	60.2
Sm	11.3	12.2	12.3	10.9	10.8	10.4	16.2	10.6	5.2	17	8.7
Eu	1.17	0.21	0.75	1.14	1.5	1.63	0.64	0.68	0.25	0.84	0.44
Gd	10.4	13.9	11.7	9.7	9.7	9.8	11.8	8.4	4.7	15.1	6.4
Tb	1.7	2.6	2.1	1.7	1.6	1.6	1.8	1.4	0.9	2.4	1
Dy	10.4	17	13.9	9.9	9.6	9.7	10.2	8.6	5.8	14.8	6.2
Ho	2.1	3.5	3	1.9	1.9	1.9	2	1.8	1.3	3	1.3
Er	6	10.4	8.9	5.6	5.7	5.4	5.8	5.4	4.2	8.5	3.9
Tm	0.9	1.59	1.43	0.84	0.84	0.81	0.86	0.86	0.73	1.21	0.61
Yb	6.1	10.1	9.6	5.5	5.7	5.3	5.5	5.8	5.2	7.8	4.3
Lu	0.91	1.48	1.47	0.84	0.88	0.83	0.82	0.86	0.84	1.13	0.66
ΣREE	357.2	274.9	429.2	334.0	539.5	320.1	830.7	369.5	168.8	472.0	473.5
$(La/Yb)_N$	8.8	3.1	6.9	9.0	28.3	12.1	27.7	10.2	4.7	8.6	20.4
$(La/Sm)_N$	4.3	2.4	4.9	4.2	5.9	4.5	8.6	5.1	4.3	3.6	9.3
$(Gd/Yb)_N$	1.4	1.1	1.0	1.4	2.7	1.7	1.7	1.2	0.7	1.6	1.2
Eu/Eu*	0.33	0.05	0.19	0.34	0.52	0.24	0.14	0.22	0.15	0.16	0.18
ASI	1.03	1.02	1.02	1.02	1.00	0.97	0.99	1.03	1.01	0.94	1.04

$Eu/Eu^* = Eu_N/(Sm_N \times GdN)^{1/2}$.

fractionated ($(La/Yb)_N$ = 4.7–27.7) than those of the Harsora granites ($(La/Yb)_N$ = 3.1–10.1). The granites of both plutons also show nearly flat HREE profiles (average $(Gd/Yb)_N$ = 1.4; Table 1) and moderate to strong negative Eu spikes, for example, Harsora: Eu/Eu* = 0.05–0.49. In the multielement spider diagram (Figure 4 *b*), the granites display prominent negative spikes in Ba, Nb–Ta, Sr–Eu, P and Ti, which may be ascribed to the fractionation of K-feldspar and/or biotite, rutile, plagioclase, apatite and titanite, respectively at some stage in the history of the source or magma[38].

The ASI (molar $Al_2O_3/(CaO–3.3P_2O_5 + Na_2O + K_2O)$, corrected for the CaO content of apatite)[39] values of the granites from two plutons are overlapping and varies from

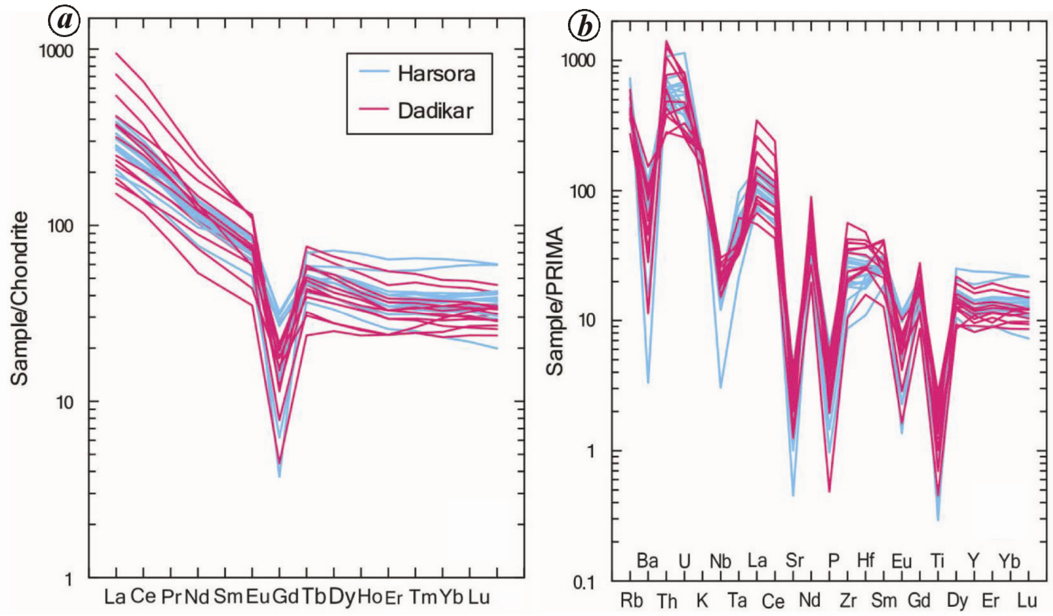

Figure 4. (***a***) Chondrite-normalized REE and (***b***) Primitive mantle (PRIMA)-normalized multi-element diagrams for the Harsora and Dadikar granites. The normalizing values in both diagrams are after McDonough and Sun[56].

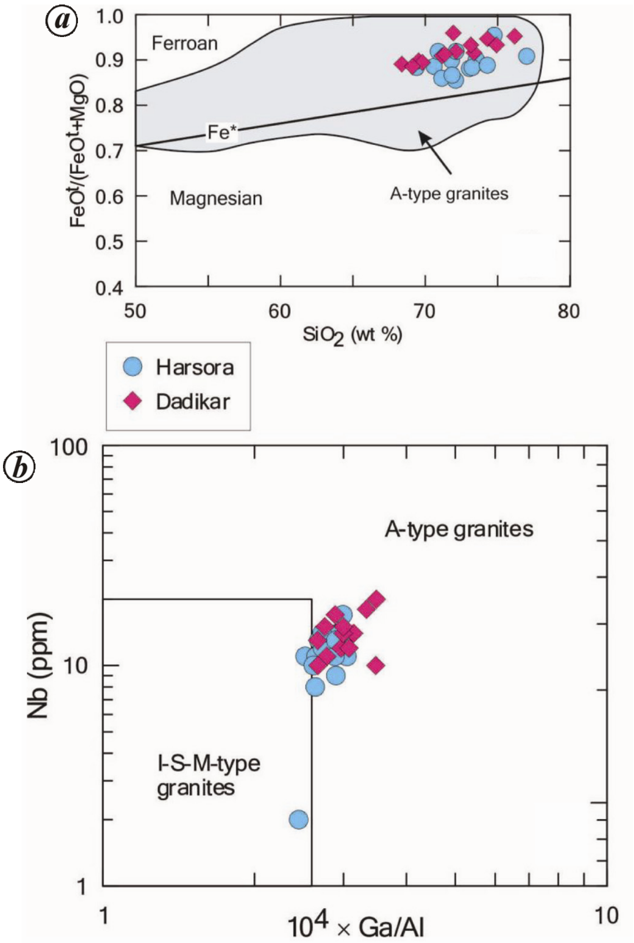

Figure 5. ***a***, $FeO^t/(FeO^t + MgO)$ versus SiO_2 (wt%) classification diagram[40]. The Fe-number (Fe*) dividing line is after Frost and Frost[57]. ***b***, Nb (ppm) versus $10^4 \times Ga/Al$ classification diagram of Whalen *et al.*[58].

0.92 to 1.06 (Table 1), suggesting that the granites are metaluminous to slightly peraluminous. The granites are ferroan and fall in the field of A-type ferroan granites (Figure 5 *a*) as per the classification scheme of Frost *et al.*[40]. Their A-type affinity is also confirmed by the Nb values and Ga/Al ratios (Figure 5 *b*), and by the presence of Fe-rich mafic minerals[8]. Eby[9] subdivided A-type granites into two chemical groups of different sources and tectonic environments. The granites of A_1 group were generated from an OIB-like source via differentiation of basaltic magma in a true anorogenic setting, whereas those of A_2 group were formed from the continental crust in post-collision or post-orogenic extensional environment. Both Harsora and Dadikar granites form a tight cluster within the field of A_2 granites in a Y–Nb–3Ga ternary diagram (Figure 6 *a*) and their Y/Nb and Yb/Ta ratios also confirm these rocks as A_2 granites (Figure 6 *b*), which are likely to form in post-collisional or post-orogenic extensional setting. The granites plot at the triple junction of syn-collision-volcanic arc-within plate-granites in the Rb versus Y + Nb diagram (Figure 7) of Pearce *et al.*[41], which is a characteristic feature of post-collision magmatism[42]. The post-collision setting of these granites is also indicated by their high alkalis, FeO^t, Zr, Y, and low Sr, CaO and MgO abundances[43]. The negative Nb anomaly, which is also the characteristic feature of most subduction-related magmas, is attributed to the preferred retention of Nb in residual titanite in the subducted slab or mantle wedge[44]. This possibility is not valid in the present scenario because the granitoids were generated in an extensional regime rather than in a subduction-related setting. Moreover, the negative Nb anomaly is also interpreted as a consequence of crustal contamination of mantle melts[38,45]. This is also not applicable to the studied A_2-type granites, which are formed from crustal-derived magmas[9].

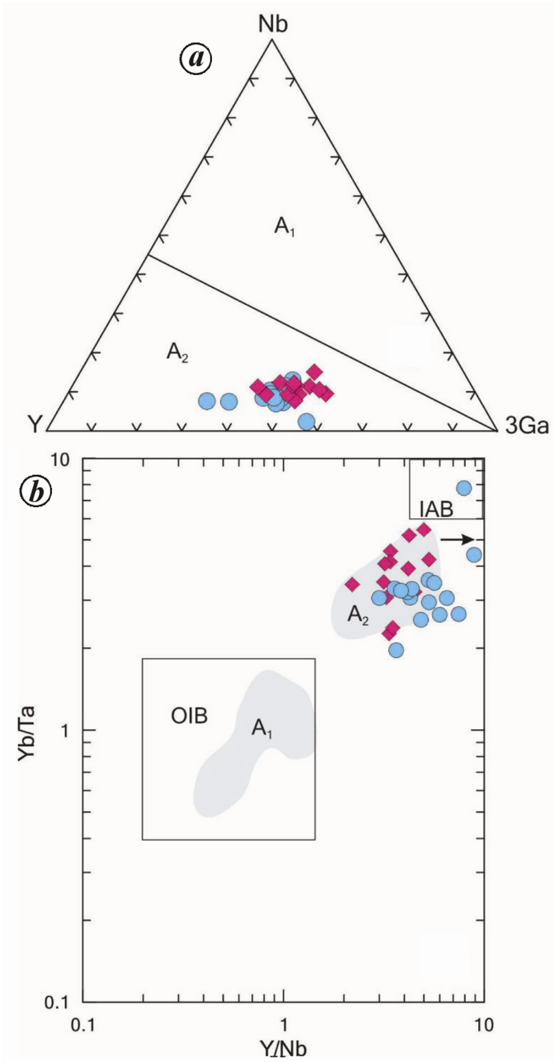

Figure 6. (*a*) Y-Nb-3Ga ternary and (*b*) Y/Nb versus Yb/Ta diagrams of Eby[9].

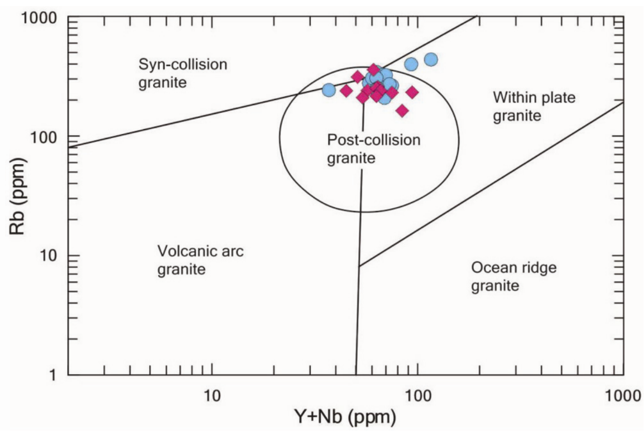

Figure 7. Rb (ppm) versus Y + Nb (ppm) tectonic discrimination diagram[41]. Field of post-collision granites is after Pearce[42].

The northern India, including the Aravalli orogen as well as the Lesser Himalaya, experienced an Andean-type subduction related magmatism at ca. 1.85 Ga, the timing of which is correlatable with the assembly of Columbia supercontinent[46–50]. The next phase of magmatic activity recorded in the Aravalli orogen is the 1.72–1.70 Ga A-type magmatism[14,18,19]. The relaxation phase following collision is often referred to as post–collisional period characterized by voluminous magmatism, whereas the within-plate settings are characterized by sparse but widespread magmatism[51]. Therefore, the gap in plutonism between 1.85 and 1.72 Ga in the Aravalli orogen probably represents a time span from subduction to post-collision, including the main phase of collision. Thus the Alwar granites may further record a case of A-type magmatism in post-collisional extensional environment and signify that A-type granites may not be restricted to anorogenic setting. These results provide a new dimension to the understanding of palaeoproterozoic crustal evolution in the Aravalli orogen. Furthermore, crustal anatexis triggered by hot mantle-derived underplated magma is considered as the most favourable process of A-type magma generation in post-collisional extensional setting[11,52–54]. The contribution of mantle melts in the generation of A-type magmas is still not well understood. Based on the above arguments in conjunction with coeval nature of A-type granites of Alwar and Khetri complexes, it is envisaged that crustal reworking was a dominant process during 1.72–1.70 Ga in the northern Aravalli orogen. This possibility should be further explored by radiogenic isotopic studies, in particular Lu–Hf isotope system.

1. Patiño Douce, A. E., What do experiments tell us about the relative contributions of crust and mantle to the origin of granitic magmas? In *Understanding Granites: Integrating New and Classical Techniques* (eds Castro, A., Fernandez, C. and Vigneresse, J. L.), Geol. Soc. London, Specl. Publ., 1999, vol. 168, pp. 55–75.
2. Condie, K. C., *Earth as an Evolving Planetary System*, Elsevier, Amsterdam, 2011, p. 574.
3. Chappell, B. W. and White, A. J. R., Two contrasting granite types. *Pacific Geol*., 1974, **8**, 173–174.
4. Loiselle, M. C. and Wones, D. R., Characteristics of anorogenic granites. *Geol. Soc. Am. Abstr. Prog.*, 1979, **11**, 468.
5. White, A. J. R., Sources of granitic magma. *Geol. Soc. Am. Abstr. Prog.*, 1979, **11**, 539.
6. Frost, C. D., Frost, B. R., Chamberlain, K. R. and Edwards, B. R., Petrogenesis of the 1.43 Ga Sherman batholith, SE Wyoming, USA: a reduced rapakivi-type anorogenic granite. *J. Petrol*., 1999, **40**, 1771–1802.
7. Bonin, B., A-type granites and related rocks: evolution of a concept, problems and prospects. *Lithos*, 2007, **97**, 1–29.
8. Eby, G. N., A-type granitoids; a review of their occurrence and chemical characteristics and speculations on their petrogenesis. *Lithos*, 1990, **26**, 115–134.
9. Eby, G. N., Chemical subdivision of the A-type granitoids: petrogenetic and tectonic implications. *Geology*, 1992, **20**, 641–644.
10. Turner, S. P., Foden, J. D. and Morrison, R. S., Derivation of some A-type magmas by fractionation of basaltic magma: an example from the Padthaway Ridge, South Australia. *Lithos*, 1992, **28**, 151–179.

11. Zhao, X. F., Zhou, M. F., Li, J. W. and Wu, F. Y., Association of Neoproterozoic A- and I-type granites in South China: implications for generation of A-type granites in a subduction-related environment. *Chem. Geol*., 2008, **257**, 1–15.
12. Mushkin, A., Navon, O., Halicz, L., Hartmann, G. and Stein, M., The petrogenesis of A-type magmas from the Amram Massif, southern Israel. *J. Petrol*., 2003, **44**, 815–832.
13. Pandit, M. K. and Khatatneh, M. K., Geochemical constraints on anorogenic felsic plutonism in North Delhi Fold Belt, western India. *Gondwana Res*., 1998, **2**, 247–255.
14. Biju-Sekhar, S., Yokoyama, K., Pandit, M. K., Okudaira, T., Yoshida, M. and Santosh, M., Late Paleoproterozoic magmatism in Delhi Fold Belt, NW India and its implication: evidence from EPMA chemical ages of zircons. *J. Asian Earth Sci*., 2003, **22**, 189–207.
15. Kaur, P., Chaudhri, N. and Hofmann, A. W., New evidence for two sharp replacement fronts during albitization of granitoids from northern Aravalli orogen, northwest India. *Int. Geol. Rev*., 2015, **57**, 1660–1685.
16. Chaudhri, N., Kaur, P., Okrusch, M. and Schimrosczyk, A., Characterisation of the Dabla granitoids, North Khetri Copper Belt, Rajasthan, India: evidence of bimodal anorogenic felsic magmatism. *Gondwana Res*., 2003, **6**, 879–895.
17. Kaur, P., Chaudhri, N., Okrusch, M. and Koepke, J., Palaeoproterozoic A-type felsic magmatism in the Khetri Copper Belt, Rajasthan, northwestern India: petrologic and tectonic implications. *Mineral. Petrol*., 2006, **87**, 81–122.
18. Kaur, P., Chaudhri, N., Raczek, I., Kröner, A. and Hofmann, A. W., Geochemistry, zircon ages and whole-rock Nd isotopic systematics for Palaeoproterozoic A-type granitoids in the northern part of the Delhi belt, Rajasthan, NW India: implications for late Palaeoproterozoic crustal evolution of the Aravalli craton. *Geol. Mag*., 2007, **144**, 361–378.
19. Kaur, P., Chaudhri, N., Raczek, I., Kröner, A., Hofmann, A. W. and Okrusch, M., Zircon ages of late Palaeoproterozoic (ca. 1.72–1.70 Ga) extension-related granitoids in NE Rajasthan, India: regional and tectonic significance. *Gondwana Res*., 2011, **19**, 1040–1053.
20. Kaur, P., Chaudhri, N., Hofmann, A. W., Raczek, I., Okrusch, M., Skora, S. and Koepke, J., Metasomatism of ferroan granites in the northern Aravalli orogen, NW India: geochemical and isotopic constraints, and its metallogenic significance. *Int. J. Earth Sci*., 2014, **103**, 1083–1112.
21. Kaur, P., Chaudhri, N., Biju-Sekhar, S. and Yokoyama, K., Electron probe micro analyser chemical zircon ages of the Khetri granitoids, Rajasthan, India: records of widespread late Palaeoproterozoic extension-related magmatism. *Curr. Sci*., 2006, **90**, 65–73.
22. Heron, A. M., The geology of northeastern Rajasthan and adjacent districts. *Mem. Geol. Surv. India*, 1917, **45**, 128.
23. Singh, S. P., Stratigraphy and sedimentation pattern in the Proterozoic Delhi Supergroup, northwestern India. In *Precambrian of the Aravalli Mountain, Rajasthan, India* (ed. Roy, A. B.), Mem. Geol. Soc. India, 1988, vol. 7, pp. 193–205.
24. Das, A. R., Geometry of the superposed deformation in the Delhi Supergroup rocks, North of Jaipur, Rajasthan. In *Precambrian of the Aravalli Mountain, Rajasthan, India* (ed. Roy, A. B.), Mem. Geol. Soc. India, 1988, vol. 7, pp. 257–266.
25. Gangopadhyay, P. K. and Sen, R., Trend of regional metamorphism: an example from 'Delhi System' of rocks occurring around Bairawas, north-eastern Rajasthan, India. *Geol. Rdsch*., 1972, **61**, 270–281.
26. Sharma, R. S., Patterns of metamorphism in the Precambrian rocks of the Aravalli mountain belt. In *Precambrian of the Aravalli Mountain, Rajasthan, India* (ed. Roy, A.B.), Mem. Geol. Soc. India, 1988, vol. 7, pp. 33–76.
27. Das Gupta, S. P., The structural history of the Khetri Copper Belt, Jhunjhunu and Sikar districts, Rajasthan. *Mem. Geol. Surv. India*, 1968, vol. 98, p. 170.
28. Lal, R. K. and Shukla, R. S., Low-pressure regional metamorphism in the northern portion of the Khetri Copper Belt, Rajasthan, India. *N. J. Miner. Abh*., 1975, **124**, 294–325.
29. Sarkar, S. C. and Dasgupta, S., Geologic setting, genesis and transformation of the sulfide deposits in the northern part of the Khetri copper belt, Rajasthan, India – an outline. *Miner. Deposita*, 1980, **15**, 117–137.
30. Lal, R. K. and Ackermand, D., Phase petrology and polyphase andalusite-sillimanite type regional metamorphism in pelitic schist of the area around Akwali, Khetri Copper Belt, Rajasthan, India. *N. J. Miner. Abh*., 1981, **141**, 161–185.
31. Naha, K., Mukhopadhyay, D. K. and Mohanty, R., Structural evolution of the rocks of the Delhi Group around Khetri, northeastern Rajasthan. In *Precambrian of the Aravalli Mountain, Rajasthan, India* (ed. Roy, A. B.), Mem. Geol. Soc. India, 1988, vol. 7, pp. 207–245.
32. Gupta, P., Guha, D. B. and Chattopadhyay, B., Basement-cover relationship in the Khetri Copper Belt and the emplacement mechanism of the granite massifs, Rajasthan. *J. Geol. Soc. India*, 1998, **52**, 417–432.
33. Gangopadhyay, P. K. and Das, D., Dadikar granite: a study on a Precambrian intrusive body in relation to structural environmental in north-eastern Rajasthan. *J. Geol. Soc. India*, 1974, **15**, 189–199.
34. Kaur, P., Chaudhri, N., Hofmann, A. W., Raczek, I., Okrusch, M., Skora, S. and Baumgartner, L. P., Two-stage, extreme albitization of A-type granites from Rajasthan, NW India. *J. Petrol*., 2012, **53**, 919–948.
35. Kaur, P., Zeh, A., Chaudhri, N., Gerdes, A. and Okrusch, M., Archaean to Palaeoproterozoic crustal evolution of the Aravalli orogen, NW India, and its hinterland: the U–Pb and Hf isotope record of detrital zircon. *Precambr. Res*., 2011, **187**, 155–164.
36. Streckeisen, A., To each plutonic rock its proper name. *Earth-Sci. Rev*., 1976, **12**, 1–33.
37. Barker, F., Trondhjemites: definition, environment and hypothesis of origin. In *Trondhjemites, Dacites and Related Rocks* (ed. Barker, F.), Elsevier, Amsterdam, 1979, pp. 1–12.
38. Tarney, J. and Jones, C. E., Trace element geochemistry of orogenic igneous rocks and crustal growth models. *J. Geol. Soc. London*, 1994, **151**, 855–868.
39. Shand, S. J., *Eruptive Rocks*, John Wiley and Sons, New York, 1949, p. 488.
40. Frost, B. R., Barnes, C. G., Collins, W. J., Arculus, R. J., Ellis, D. J. and Frost, C. D., A geochemical classification for granitic rocks. *J. Petrol*., 2001, **42**, 2033–2048.
41. Pearce, J. A., Harris, N. B. W. and Tindle, A. G., Trace element discrimination diagrams for the tectonic interpretation of granitic rocks. *J. Petrol*., 1984, **25**, 956–983.
42. Pearce, J. A., Sources and settings of granitic rocks. *Episodes*, 1996, **19**, 120–125.
43. Rogers, J. J. W. and Greenberg, J. K., Late-orogenic, post-orogenic, and anorogenic granites; distinction by major-element and trace-element chemistry and possible origins. *J. Geol*., 1990, **98**, 291–308.
44. Saunders, A. D., Tarney, J. and Weaver, S. D., Transverse variations across the Antarctic Peninsula: implications for the genesis of calc-alkaline magmas. *Earth Planet. Sci. Lett*., 1980, **46**, 344–360.
45. Herget, J. M., Chappell, B. W., McCulloch, M. T., McDougall, I. and Chivas, A. R., Geochemical and isotopic constraints on the origin of the Jurassic dolerites of Tasmania. *J. Petrol*., 1989, **30**, 841–883.
46. Kaur, P., Chaudhri, N., Raczek, I., Kröner, A. and Hofmann, A. W., Record of 1.82 Ga Andean-type continental arc magmatism in

NE Rajasthan, India: insights from zircon and Sm–Nd ages, combined with Nd–Sr isotope geochemistry. *Gondwana Res.*, 2009, **16**, 56–71.

47. Kaur, P., Zeh, A., Chaudhri, N., Gerdes, A. and Okrusch, M., Nature of magmatism and sedimentation at a Columbia active margin: insights from combined U–Pb and Lu–Hf isotope data of detrital zircons from NW India. *Gondwana Res.*, 2013, **23**, 1040–1052.
48. Kohn, M. J., Paul, S. K. and Corrie, S. L., The lower Lesser Himalayan sequence: a Paleoproterozoic arc on the northern margin of the Indian plate. *Bull. Geol. Soc. Am.*, 2010, **122**, 323–335.
49. Bhowmik, S. K. and Dasgupta, S., Tectonothermal evolution of the Banded Gneissic Complex in central Rajasthan, NW India: present status and correlation. *J. Asian Earth Sci.*, 2012, **49**, 339–348.
50. Ozha, M. K., Mishra, B., Hazarika, P., Jeyagopal, A. V. and Yadav, G. S., EPMA monazite geochronology of the basement and supracrustal rocks within Pur-Banera basin, Rajasthan: evidence of Columbia breakup in Northwestern India. *J. Asian Earth Sci.*, 2016, **117**, 284–303.
51. Bonin, B., Do coeval mafic and felsic magmas in post-collisional to within-plate regimes necessarily imply two contrasting, mantle and crustal, sources? A review. *Lithos*, 2004, **78**, 1–24.
52. Yang, J. H., Wu, F. Y., Chung, S. L., Wilde, S. A. and Chu, M. F., A hybrid origin for the Qianshan A-type granite, northeast China: geochemical and Sr–Nd–Hf isotopic evidence. *Lithos*, 2006, **89**, 89–106.
53. Ma, C. Q., Li, Z. C., Ehlers, C., Yang, K. G. and Wang, R. J., A post-collisional magmatic plumbing system: mesozoic granitoid plutons from the Dabieshan high pressure and ultrahigh-pressure metamorphic zone, east-central China. *Lithos*, 1998, **45**, 431–456.
54. Mo, X. X. *et al.*, Mantle contributions to crustal thickening during continental collision: evidence from Cenozoic igneous rocks in southern Tibet. *Lithos*, 2007, **96**, 225–242.
55. Singh, S. P., Sedimentation patterns of the Proterozoic Delhi Supergroup, northeastern Rajasthan, India, and their tectonic implications. *Sediment. Geol.*, 1988, **58**, 79–94.
56. McDonough, W. F. and Sun, S.-S., Composition of the Earth. *Chem. Geol.*, 1995, **120**, 223–253.
57. Frost, B. R. and Frost, C. D., A geochemical classification for feldspathic igneous rocks. *J. Petrol.*, 2008, **49**, 1955–1969.
58. Whalen, J. B., Currie, K. L. and Chappell, B. W., A-type granites, geochemical characteristics, discrimination and petrogenesis. *Contrib. Miner. Petrol.*, 1987, **95**, 407–419.

ACKNOWLEDGEMENTS. We thank two anonymous reviewers, and Prof. N. V. Chalapathi Rao for their valuable comments that improved the final version of the manuscript. We also thank Jaideep Tiwana for assistance in sample preparation.

Received 25 May 2016; revised accepted 20 August 2016

doi: 10.18520/cs/v112/i03/608-615

Conservation of jack wood (*Artocarpus heterophyllus* Lamk.) sculptures in an ancient temple in Kerala, South India: identification of heritage wood samples, neem gum–cashew nut shell liquid application in consolidation and preservation

M. P. Sujith[1], L. Rajeswari[1], T. Sreelakhmi[1] and E. V. Anoop[2,*]

[1]Archaeological Survey of India, Thrissur Circle, Purathathva Bhavan, Pullazhy, Thrissur 680 012, India
[2]Department of Wood Science, College of Forestry, Kerala Agricultural University, Thrissur 680 656, India

This present communication deals with the anatomical identification of wood samples of an ancient archaeological monument in India, Sri Vishnu temple, Kadavallur in Thrissur (Kerala) and the consolidation of fissures and cracks formed due to seasoning over a period of time using neem gum and preservation using cashew nut shell liquid extract. Neem gum which has anti-bacterial qualities and CNSL organic extract which has anti-termite and anti-fungal preservative action are found suitable for conservation and preservation of these sculptures. The active ingredient in organic preservative, CNSL, was analysed using HPLC and compared using UV spectra. The peaks of monoene, diene and triene in anachardic acid are visible in the spectra. The preservative, CNSL, also enhanced the aesthetic appeal of the jack wood sculptures. CNSL-coated jack wood had lower moisture absorption as demonstrated by Karsten tube experiment. The results imply that the strength of the material formed out of neem gum and wood powder used for filling of cracks and fissures can be modified as per requirement using distilled water and that the application is reversible. This method of conservation was found suitable under warm and humid conditions to which these sculptures are subjected to.

Keywords: Conservation, CNSL, heritage wood, preservation, wooden sculptures.

THE dexterous consolidation and filling up of cracks finds much application in heritage sculptures. In the case of conservation of wooden sculptures the present methods largely depend on synthetic adhesives like cyanoacrylates and epoxy resins. The low compatibility and irreversibility of these materials and their synthetic nature make them less attractive for heritage conservation. Traditionally, the temples and other ancient structures of Kerala

*For correspondence. (e-mail: anoop.ev@kau.in)